Parametrization of the Nonevasive Exchange Processes and Background Contributions in the Reaction $\pi^- p \to n\pi^+\pi^-$ at 2.77 GeV/c

L. D. Jacobs*
Département de Physique des Particules Elémentaires, CEN-Saclay, F-91 Gif-sur-Yvette, France
(Received 31 January 1972)

An analysis of 20 000 events from the reaction $\pi^- p \to n\pi^+\pi^-$ at 2.77 GeV/c is performed according to a parametrization given by Froggatt and Morgan. With reasonable assumptions as to the form of the s-wave $\pi\pi$ amplitude, we are able to reproduce the low-t behavior of the mean moments and differential cross section after obtaining best values for the parameters $\Gamma_l^{s,p}$ in a maximum-likelihood fit. The method may be termed nonevasive. Some discussion is presented on the validity of evasive extrapolation.

INTRODUCTION

In recent years much interest has been given to the question of treating the data from the reaction $\pi N \to N\pi\pi$ at low values of t, momentum transfer squared. More than sufficient reason exists for working within the framework of one-pion exchange (OPE) to the extent that OPE has gone beyond the strict assumption of a model and come to be regarded as an accepted physical explanation. No such agreement, however, applies to the question of describing the corrections to OPE at low t and how these corrections behave as t goes into the unphysical region towards the pion pole. While the need to correct OPE is undisputed, especially in its failure to describe the decay density-matrix elements as functions of t, contention has arisen on (i) reconciling the data on $\pi N \to N\pi\pi$ with the predictions from the reaction $\gamma N \to N\pi$, via the vector-dominance model, that transversely polarized ρ's peak in the forward direction,[1] and (ii) whether the "off-shell" $\pi\pi$ cross-section function

$$F_0(m,t) = \frac{2\pi}{f^2} \frac{P_{\rm lab}{}^2}{m(m^2-4\mu^2)^{1/2}} (t-\mu^2)^2 \frac{\partial^2\sigma}{\partial t \partial m^2} \quad (1)$$

as well as the functions

$$F_l(m,t) = \frac{2\pi}{f^2} \frac{P_{\rm lab}{}^2}{m(m^2-4\mu^2)^{1/2}} (t-\mu^2)^2 \times \frac{1}{\sqrt{4\pi}} \int \frac{\partial^3\sigma}{\partial t \partial m^2 \partial\Omega} Y_{l0}(\Omega) d\Omega \,, \quad (2)$$

$l = 1, 2$, vanish at $t = 0$.[2] m is the dipion mass, and $\Omega = (\cos\theta, \phi)$ describes the decay directions.

In the reaction $\pi^- p \to n\pi^+\pi^-$ the problem is rendered more complicated and, of course, more interesting, by the presence of the large s-wave $\pi\pi$ amplitude in addition to the ρ amplitude. It is important to understand the low-t region, for, by a process of extrapolating to the pion pole, it is possible to obtain values of the constituent $\pi\pi$ phase shifts, and in particular $\delta_{I=0}^{I=0}$.

The emphasis in the present paper is on the selection and use of a good parametrization of the low-t behavior in the events coming from the reaction $\pi^- p \to n\pi^+\pi^-$. At the same time, we include in our fitting procedure in a simplified fashion ρ production at higher values of t, f^0 production, and nucleon resonance production. We have tried to reproduce the complete 4-dimensional (t, m, Ω) spectrum. Thus, in the fitting programs we use the complete sample of events, but we restrict our discussion and presentation in the main to events with $|t| \leq 20\mu^2$.

METHOD OF ANALYSIS

The sample of events in the analysis are the 20 000 fitting the hypothesis $\pi^- p \to n\pi^+\pi^-$ in a Saclay hydrogen bubble chamber experiment at 2.77 GeV/c. Details of the experiment in which the pictures were produced will be found elsewhere.[3]

We have adopted an iterative scheme based on three well-known programs which have been extensively modified for our purposes, viz., MURTLEBERT,[4] FOWL,[5] and KIOWA[6]. MURTLEBERT optimizes the parameters of the current set of hypotheses by a maximum-likelihood method. We use the parameters of the fit to generate Monte Carlo events in FOWL and make a direct comparison between the experimental histograms and theoretical distributions and scatter plots. In KIOWA, we weight each experimental event by the inverse of the total matrix element squared and plot suitable histograms. It is evident that when we have arrived at a faithful representation of the channel, the FOWL distributions will reproduce the experimental distributions and, what is perhaps more interesting, all the KIOWA distributions will follow phase space. Alternatively, if in addition we weight by the inverse of phase space, t distribu-

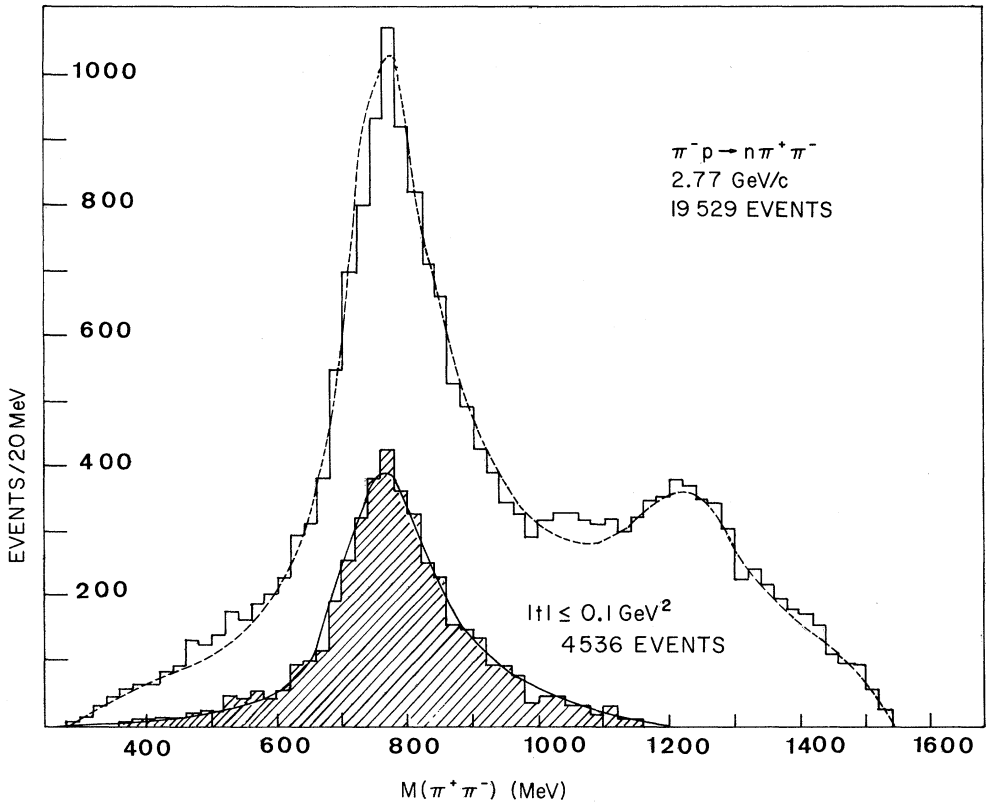

FIG. 1. $\pi^+\pi^-$ mass spectrum for all t and for $|t| \leq 0.1$ GeV^2, shown hatched. Dashed curve shows fit with parameters shown in Tables I and II. Solid curve is corresponding curve for $|t| < 0.1$ GeV^2.

tions, for example, will be uniform. In the absence of this felicitous state of affairs, we examine the distributions to see where the fit is lacking, and in particular to see whether events are accounted for in various kinematic regions. We use this knowledge to modify the hypotheses for input into MURTLEBERT.

Our final choice of hypotheses consists of a term that describes peripheral production of a dipion state where we have allowed the dipion to have angular momentum 0 and 1, plus terms describing the other processes. These terms are added incoherently and from our point of view take account of a background whose presence can be detected at $|t| \gtrsim 7\mu^2$ and which becomes important for $|t| \sim 20\mu^2$. The actual parametrization of these background terms at large t is left until we complete the discussion of the dominant process. In Fig. 1, however, we present the over-all $\pi\pi$ mass spectra for all t and $|t| \leq 4\mu^2$ in order to show how successful the fit is. It is good everywhere except in the region of 1100 MeV. This region is known to have interesting effects; we are content to say that our analysis has shown an anomaly to be present, i.e., an effect outside the assumptions we have made. At 500 MeV there appears to be an excess of events but not at low values of t.

NONEVASIVE PARAMETRIZATION OF HELICITY AMPLITUDES

Froggatt and Morgan (FM) have written down t-channel helicity amplitudes which in the low-t region approximate those invariant amplitudes having kinematic singularities at $t=0$ and $t=t_{\min}$ under the appropriate constraints.[7,8] That is to say, they are correlated, so that despite these singularities in the individual amplitudes, the intensity functions are nonsingular. To try to extend the validity of the FM parametrization beyond the low-t region ($t \leq 4\mu^2$), we include factors $\alpha_i(t)$ which are exponential in t and can differ one from another at large values of t. They govern the behavior of $d\sigma/dt$ and $(d\sigma/dt)\langle Y_{lm}(\Omega)\rangle$. They are to be regarded as phenomenological terms as required by the data and in no way are they supposed to correct for any off-shell factor elsewhere in the calculation. The modified FM amplitudes are

$$f^{s,p}_{\frac{1}{2}\frac{1}{2}00} = a^{s,p}_{\pi\pi}\alpha_0^{s,p}(t)\left(\frac{\sqrt{-t}}{t-\mu^2} + \frac{\Gamma_0^{s,p}}{\sqrt{-t}}\right), \tag{3}$$

$$f^{s,p}_{\frac{1}{2}-\frac{1}{2}:00} = a^{s,p}_{\pi\pi}\alpha^{s,p}_0(t)\frac{\Gamma^{s,p}_0}{\sqrt{-t}}\left(\frac{t}{t_{\min}}-1\right)^{1/2}, \quad (4)$$

$$f^{p}_{\frac{1}{2}\frac{1}{2}:\pm 10} = \pm a^{p}_{\pi\pi}\alpha^{p}_1(t)\frac{\Gamma^{p}_1}{\sqrt{-t}}\left(\frac{t}{t_{\min}}-1\right)^{1/2}, \quad (5)$$

$$f^{p}_{-\frac{1}{2}-\frac{1}{2}:\pm 10} = a^{p}_{\pi\pi}\alpha^{p}_1(t)\frac{\Gamma^{p}_1}{\sqrt{-t}}\left(\frac{t}{t_{\min}}-1\right)^{1/2}, \quad (6)$$

where

$$a^{s}_{\pi\pi} = \tfrac{2}{3}e^{i\delta^0_0}\sin\delta^0_0 + \tfrac{1}{3}e^{i\delta^2_0}\sin\delta^2_0, \quad (7)$$

$$a^{p}_{\pi\pi} = 3e^{i\delta_1}\sin\delta_1, \quad (8)$$

$$\alpha^{s,p}_i(t) = \exp\tfrac{1}{2}[A^{s,p}_i(t-\mu^2) + B^{s,p}_i(t-\mu^2)^2]. \quad (9)$$

We have, therefore,

$$\frac{\partial\sigma}{\partial t\partial m^2\partial\Omega} = \tfrac{1}{2}C\sum_{\lambda\lambda'}\left|f^{s}_{\lambda\lambda'} + \sum_{\nu} f^{p}_{\lambda\lambda':\nu_0}Y_{1\nu}(\Omega)\right|^2, \quad (10)$$

where C, the kinematic constant, is

$$C = \frac{m}{k}\frac{f^2}{2\pi P_{\rm lab}{}^2\mu^2}. \quad (11)$$

In addition we may use the above set of amplitudes to derive expressions for the "off-shell" functions (1) and (2) in terms of the $\Gamma^{s,p}_i$. For simplicity in the presentation of the formulas we take $\alpha^{s,p}_i(t) = 1$:

$$F_0(m,t) = \frac{|a^{s}_{\pi\pi}|^2}{\mu^2k^2}\left[-t + 2(t-\mu^2)\Gamma^{s}_0 + (t-\mu^2)^2\frac{(\Gamma^{s}_0)^2}{-t_{\min}}\right] + \frac{|a^{p}_{\pi\pi}|^2}{3\mu^2k^2}\left[-t + 2(t-\mu^2)\Gamma^{p}_0 + (t-\mu^2)^2\frac{(\Gamma^{p}_0)^2 + 4(\Gamma^{p}_1)^2}{-t_{\min}}\right], \quad (12)$$

$$F_1(m,t) = \frac{2}{\sqrt{3}\,\mu^2k^2}\,\mathrm{Re}(a^{p}_{\pi\pi}a^{*s}_{\pi\pi})\left[-t + (t-\mu^2)(\Gamma^{s}_0 + \Gamma^{p}_0) + (t-\mu^2)^2\frac{\Gamma^{p}_0\Gamma^{s}_0}{-t_{\min}}\right], \quad (13)$$

$$F_2(m,t) = \frac{2|a^{p}_{\pi\pi}|^2}{3\sqrt{5}\mu^2k^2}\left[-t + 2(t-\mu^2)\Gamma^{p}_0 + (t-\mu^2)^2\frac{(\Gamma^{p}_0)^2 - 2(\Gamma^{p}_1)^2}{-t_{\min}}\right]. \quad (14)$$

For the low-t region, the important parameters at a fixed value of the mass m of the dipion system, are the three FM parameters: $\Gamma^{s,p}_i$, assumed real. We have implicitly assumed factorization and therefore it follows that all the mass dependence of the amplitudes lies in the phase shifts. However, we find a Breit-Wigner width for the ρ appreciably larger than that found in the same data by extrapolating to the π pole. This suggests that the exponential slopes in the expressions for $\alpha_i(t)$ vary with mass. Under these circumstances our results on the t variation of the mean moments $\langle Y_{lm}\rangle$ and $(d\sigma/dt)\langle Y_{lm}\rangle$ are only strictly valid in the ρ mass region.

For the phase shifts themselves, (i) for δ^2_0, we use the solutions of Baton, Laurens, and Reignier (BLR)[9]; (ii) for δ^1_1 we first used a p-wave Breit-Wigner function with the experimental resolution folded in (estimated at ±6 MeV) and finally an expression having the functional form:

$$\frac{k^{2l+1}}{m}\cot(\delta + i\epsilon) = \frac{m_0{}^2 - m^2}{\Gamma_0 m_0{}^2}\frac{k_0{}^{2l+1}(1+\alpha k^2)}{1+\beta k^2+\gamma k^4}, \quad (15)$$

where

$$k^2 = m^2 - 4\mu^2. \quad (16)$$

m_0 and Γ_0 are the mass and width of the resonance,

$$k_0{}^2 = m_0{}^2 - 4\mu^2, \quad (17)$$

and α, β, and γ are complex numbers, constrained so that for $k\to\infty$, the phase shift is purely inelastic, i.e.,

$$\delta^1_1 \to 0, \quad \epsilon^1_1 \to \infty, \quad \text{i.e.,} \quad \eta^1_1 = e^{-2\epsilon^1_1} \to 0.$$

In effect, however, the values of α and β obtained give rise to a purely elastic phase shift at our values of m; their main effect is that δ^1_1 levels off at 147° instead of 157° which we obtained with the Breit-Wigner function. (iii) For δ^0_0, we adopted the following procedure. We have taken the two sets of solutions given by BLR,[9] obtained from the same data which are designated "down-up" and "down-down." We chose convenient values of the mass m_i and set the values of δ^0_0 at each of the mass positions m_1, m_2, m_3, etc. to d_1, d_2, d_3, etc. The initial values of d_i were taken from the BLR solution, and for $m > 0.82$ MeV could be complex. To obtain values of δ^0_0 at values of m other than the m_i, we computed $(k/m)\cot d_i$ and by linear interpolation of the real and imaginary parts we obtained values of $(k/m)\cot(\delta^0_0 + i\epsilon^0_0)$ and thus the values of δ^0_0 and ϵ^0_0 and the inelasticity $\eta^0_0 = e^{-2\epsilon\delta}$. Interpolation of this function is useless when it has a singularity. This can happen at $\delta^0_0 = n\pi$. This occurs at threshold and in the "down-up" solution at $m \approx 1.05$ GeV. In the latter case, linear interpolation of δ^0_0 itself was used. We allowed for the possibility of the d_i being parameters in the fit, and, in fact, in the results that we present, we use the sets that maximize the likelihood. We do not regard our work as providing yet another set of solutions of δ^0_0, since we stay in the physical region, but since the fits did seem to be sensitive to the values of d_i input, we can have some degree of confidence

in the answer to the question, which of the two sets "down-up" or "down-down" gave the greater likelihood? We find that fits with "down-down" tended to have logarithmic likelihoods smaller by 20 than the same fit, but with the d_i replaced by the "down-up" set. However, there was a tendency to give an even better fit with a mixture of the two solutions which, of course, gives a δ_0^0 with a bizarre mass dependence. Further, the grid we use for $m_i - d_i$ is not fine enough to detect any real, violent changes in δ_0^0 such as may happen near the $K\bar{K}$ threshold. In Fig. 2 we show the values of δ_0^0 and η_0^0 used. The points give the positions $d_i - m_i$ and the two lines indicate the interpolations in the two cases. They both lie within the bands given by BLR – except that our "down-down" coincides with the "down-up" until 820 MeV. This is hardly surprising since the data are the same and we were guided in our choice of parameters by the BLR curves. What is noteworthy and, for us, gratifying, is to see that our method of analysis, which is completely different from the extrapolation procedure used to get the BLR curves, does not introduce any untoward distortions and permits us to have some degree of assurance in the analysis.

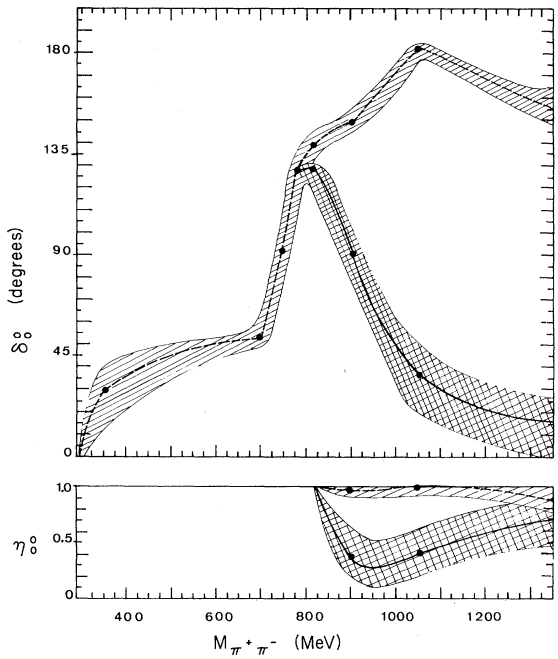

FIG. 2. $\pi\pi$ phase shift δ_0^0 and inelasticity η_0^0. The points show the final fixed values of δ_0^0 and η_0^0 used for interpolating the variation of these quantities with $M\pi^+\pi^-$. The singly hatched band shown is the "down-up" solution. The cross-hatched band is the "down-down" solution. The estimated error is of the order of width of the bands.

RESULTS OF THE ANALYSIS

Before setting out the results in detail, we will list briefly those aspects of the data where it is felt some advance in our knowledge of the reaction mechanism has been made.

(1) The three parameters $\Gamma_i^{s,p}$, which were given every freedom by the fitting program to vanish if the data so required, are found to be nonzero. A corollary of this result is that the contribution to the $\pi\pi$ cross section at $t=0$ is nonvanishing, i.e., $F_0(m, t=0) \neq 0$.

(2) While the values of $\Gamma_i^{s,p}$ are several standard deviations away from zero, they are nevertheless so small that they do not really invalidate any analysis which assumes the vanishing of $F_0(m, t=0)$.

(3) Although we show, by means of the FM formalism, that extrapolation of the asymmetry parameter is a dangerous procedure, it turns out to be valid with our choice of $\Gamma_i^{s,p}$.

TABLE I. Values of parameters used in the modified FM helicity amplitudes.

t and Ω dependence		m dependence					
			s wave[a]			p wave	
Parameter	Value	i	m_i (MeV)	d_i (deg)	ϵ_i	Parameter	Value
Γ_0^s	-0.010 ± 0.001						
Γ_0^p	-0.064 ± 0.010	1	360	30 ± 10	0	m_0	0.7735 ± 0.001
Γ_1^p	0.116 ± 0.002	2	700	52.7 ± 5	0	Γ_0	0.17835 ± 0.00025[b]
A_0^s	-0.45 ± 0.80	3	750	91.7 ± 3	0	Reα	-0.95 ± 0.08
B_0^s	19.64 ± 8.00	4	775	126.5 ± 3	0	Imα	1.15 ± 0.30
A_0^p	4.30 ± 0.20	5	820	140 ± 5	0		
				(127 ± 5)		Reβ	-1.75 ± 0.50
B_0^p	-0.09 ± 0.10	6	900	149.3 ± 7	0.0087		
		(6)	(900)	(91.4 ± 7)	(0.51 ± 0.20)		
A_1^p	7.42 ± 0.05					Imβ	0.47 ± 0.47
		7	1050	183.2 ± 5	0.0005		
B_1^p	-1.74 ± 0.15	(7)	(1050)	(36 ± 10)	(0.44 ± 0.25)		

[a] "Down-up" solutions, "down-down" solution in parentheses.
[b] Effect of resolution not subtracted.

(4) The FM formalism with the optimum parameters that we have obtained is a good description of the data at low t. In particular, it predicts that the moment $\langle Y_{22}\rangle$ in the Jackson frame should be zero, which is the case, to within the errors of the data points.

(5) As mentioned above, the "down-up" solution is preferred to the "down-down." However, we cannot completely rule out the possibility that computer approximating procedures, which are not the same in the two cases, might account for the difference, or that a change in some of our assumptions might well reverse this preference. It should be noted that when curves corresponding to the two hypotheses are drawn on histograms, or when two values of χ^2 are calculated on a scatter plot, no statistical difference is obtained.

In Table I, we show the values of $\Gamma_i^{s,p}$, $A_i^{s,p}$, and $B_i^{s,p}$ obtained and the other parameters in the fit. The errors quoted come from the fitting programs when the log likelihood is allowed to decrease by 0.5 under the assumption of a locally quadratic variation of the log likelihood function. The parameter Γ_1^p has been observed thoughout the whole fitting procedure to really have the error ascribed to it. It has been noted previously that this parameter can be well determined.[8] Its importance was first recognized by Kane and Ross,[2] when they postulated that the amplitude is predominantly helicity flip at low t. In physical terms, it measures the amount of depolarized ρ produced and it is determined by the shape of the functions $\langle Y_{21}\rangle$ and $\langle Y_{11}\rangle$ as a function of t. The parameters Γ_0^s and Γ_0^p are less reliable. They contribute together to the value of the s-p interference term, e.g., see formula (13) for $F_1(m,t)$ above, and are correlated to a certain degree. They give rise to the uncertainty in the value of $F_0(m,0)$.

Before proceeding further with the discussion of the $\Gamma_i^{s,p}$ parameters, it is as well to show how the data fit and where the shortcomings of the formalism lie. In Fig. 3, we have selected all events with m between 0.65 and 0.90 GeV and we have plotted in fine bins of 0.25 μ^2 the values of $\sqrt{4\pi}\ \langle Y_{lm}\rangle$ where $l=1, 2$, and $m=0, 1$, in the Jackson frame. (In Appendix A we give the relationship between the mean moments $\langle Y_{lm}\rangle$ and the usually defined density-matrix elements). As has already been mentioned, $\langle Y_{22}\rangle$ is compatible with zero.

There is some question of how far within the experimental resolution one can reduce the bin size in t, especially for $t\approx 0$, i.e., for very slow recoil neutrons. For a bin size of $0.25\mu^2$ we must know the lab momentum of the neutron, q, to within $\mu^2/4q$. For $t\simeq -\mu^2$ we must have $dq\simeq 35$ MeV/c. Certainly, if one is determined to investigate the low-t region, one might expect greater success and have more confidence in one's data at the com-

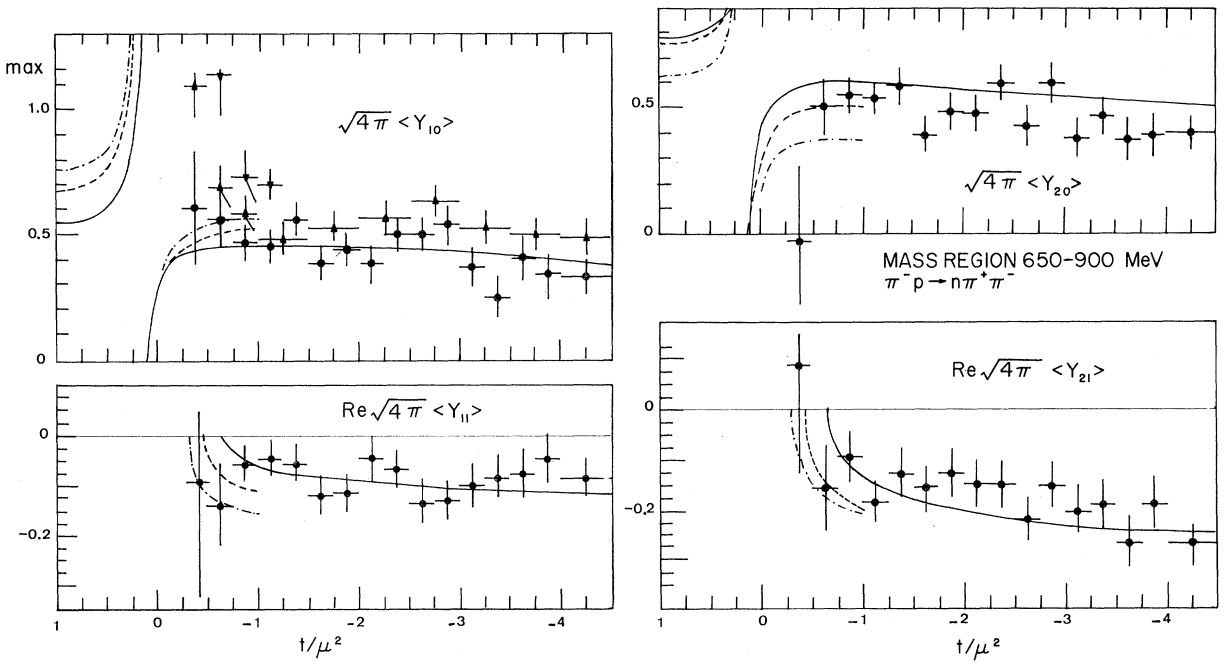

FIG. 3. Experimental values of $\sqrt{4\pi}\langle Y_{10}\rangle$, $\sqrt{4\pi}\langle Y_{20}\rangle$, $\sqrt{4\pi}\langle Y_{11}\rangle$, and $\sqrt{4\pi}\langle Y_{21}\rangle$ for the mass region 650–900 MeV. All points shown ● are from the present experiment at 2.77 GeV/c. For $\langle Y_{10}\rangle$ the points shown ▼ are from the world compilation 1.7–2.5 GeV/c and shown ▲ 2.5–3.2 GeV/c. The solid curves are the result of the fit at $M\pi\pi$= 773 MeV. The curves are also indicated for 700 MeV (dashed) and 650 MeV (dot-dashed).

paratively low energy of the present experiment, 2.77 GeV/c (where one can measure both tracks, one of which must be quite long, since they carry off the momentum of the incoming pion), than in a recent spark chamber experiment at high energy, 15 GeV/c.[10]

The points detailed by a solid black circle in Fig. 3 are our events at 2.77 GeV/c. They show that the mean moments have a slow variation with t for $t \lesssim 4\mu^2$. The solid curves are the results of the calculation at the mass of the ρ (773.5 MeV). The other curves indicate the results of the calculation near the kinematic limit for values of m at 650 and 700 MeV. As t decreases, the shape of the Chew-Low boundary allows the smallest t region to be physical only for events in the m region 650–700 MeV. Since the mass band is so wide, the curves are to be taken as showing how the variation of the moments with t appears and not as exact fits to the points.

Because they do not contain the term $(t/t_{\min}-1)^{1/2}$ the moments $\langle Y_{10}\rangle$ and $\langle Y_{20}\rangle$ remain real as t goes unphysical. We have calculated the values of these moments for t positive and for the t range 0–$1\mu^2$. The curves are displayed on the figure. Williams[11] has already shown similar curves and it is easy to appreciate how the discontinuity observed comes about. The differential cross section (DCS) dN/dt and the functions $\sqrt{4\pi}\langle Y_{10}\rangle dN/dt$, $\sqrt{4\pi}\langle Y_{20}\rangle dN/dt$ (or if one prefers, the functions F_0, F_1, and F_2) vanish in our formulation at values of t just slightly positive, but to within the errors found on the parameters $\Gamma_i^{s,p}$, at values of t which are not the same for each function. For $\langle Y_{20}\rangle$ this means that any extrapolation of the moment, if one were attempted, would be doomed to failure. For $\langle Y_{10}\rangle$, by inspection it will be seen that a straight line through the solid curve in the region $-t$, 2–$4.5\mu^2$ extrapolates at $t=\mu^2$ to the same value as is given by the solid curve, even though this has a singularity in our calculation.

In order to test the FM hypothesis further, we also made use of the 38 000 events of the well-known $\pi^- p \to N\pi\pi$ compilation.[12] For the moments $\langle Y_{20}\rangle$, $\mathrm{Re}\langle Y_{21}\rangle$, and $\mathrm{Re}\langle Y_{11}\rangle$, data from the compilation which covers the beam momentum range 1.7–3.2 GeV/c seemed within errors compatible with the data at 2.77 GeV/c and could be represented well by the curves presented in Fig. 3. For

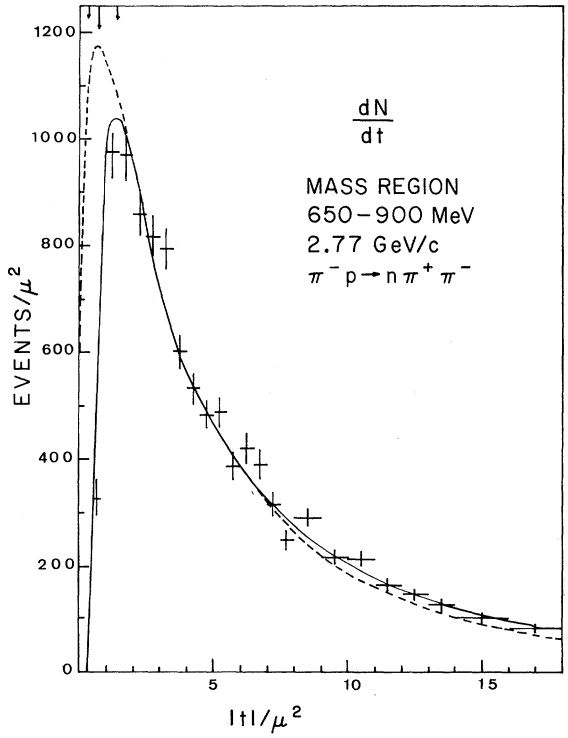

FIG. 4. Differential cross section. The three arrows indicate the kinematic limits in t at 2.77 GeV/c for m= 650, 773, and 900 MeV. The solid curve is from a Monte Carlo simulation of the fit for the 650–900-MeV mass band. The dashed curve is the computed DCS at the ρ mass using the FM hypothesis only and without the kinematic cutoff.

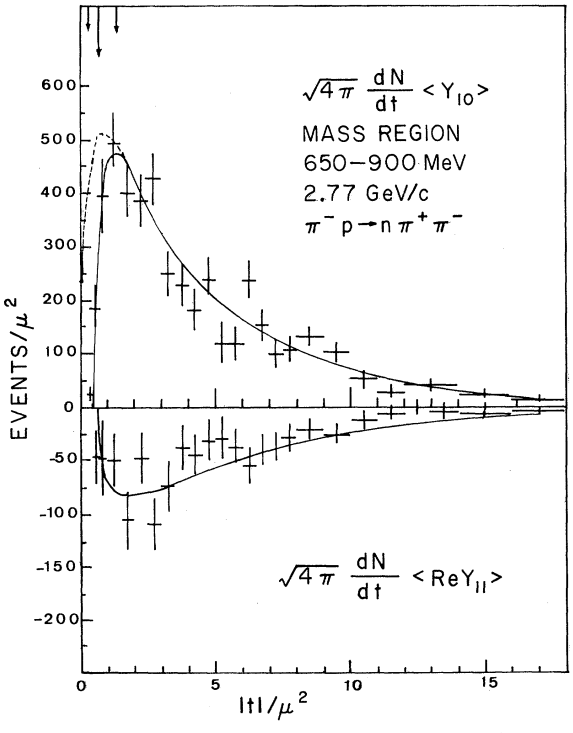

FIG. 5. Differential cross section weighted by $\sqrt{4\pi}\langle Y_{1m}\rangle$. The three arrows indicate the kinematic limits in t at 2.77 GeV/c, for m = 650, 773, and 900 MeV. The solid curve is from a Monte Carlo simulation of the fit for the 650–900-MeV mass band. The dashed curve corresponds to the value computed at the ρ mass using the FM hypothesis and is shown where it differs from the solid curve, i.e., in the unphysical region.

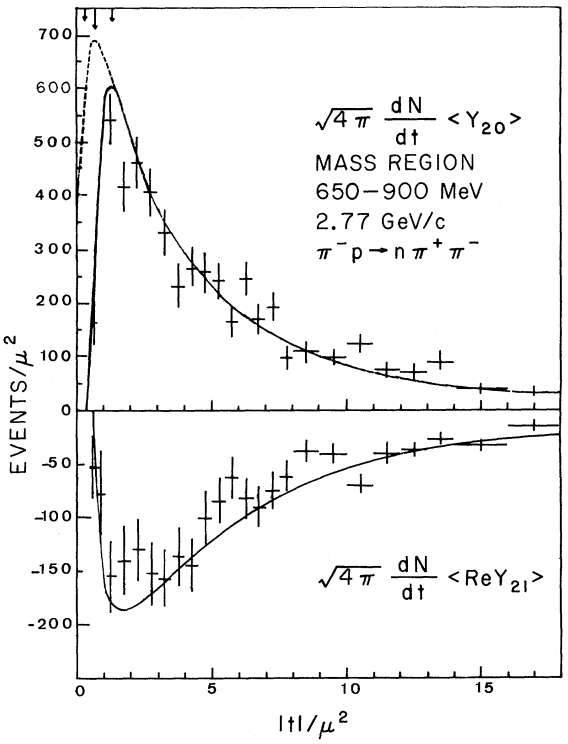

FIG. 6. Differential cross section weighted by $\sqrt{4\pi}\langle Y_{2m}\rangle$. The three arrows indicate the kinematic limits in t at 2.77 GeV/c, for m= 650, 773, and 900 MeV. The solid curve is from a Monte Carlo simulation of the fit for the 650–900-MeV mass band. The dashed curve corresponds to the value computed at the ρ mass using the FM hypothesis and is shown where it differs from the solid curve, i.e., in the unphysical region.

the moment $\langle Y_{10}\rangle$ there was compatibility of the data for $-t > \mu^2$. Since it was not possible for practical reasons to plot all the data points together, we plot only the moments $\langle Y_{10}\rangle$ for the sample of events in the compilation that spanned our beam momentum, i.e., those events in the range 2.5–3.2 GeV/c. We also plot three points at the smallest values of t, for events from the sample 1.7–2.5 GeV/c. Near the kinematic limit there appear to be divergences. The points from the compilation seem to be consistently higher than our points at 2.77 GeV/c, especially at the lower momentum. This may indicate that Γ_0^p and Γ_0^s are strongly beam-energy-dependent. In Ref. 7, FM allow for the possibility of these two parameters being complex, and they mention that there are interesting possibilities for distortions to be observed, coming from the interference of terms containing complex values of $\Gamma_0^{s,p}$ and the $\pi\pi$ scattering amplitudes.

To see how well the data fit quantatively, we must turn to Figs. 4–6, which present histograms of the events at 2.77 GeV/c, weighted by $Y_{lm}(\cos\theta, \phi)$ for each event in the 650–900-MeV mass band. Figure 4 shows the differential cross section. The dotted curve is analogous to the solid curves on Fig. 3. It corresponds to the differential cross section calculated using formula (10) with $t_{\min}$ and the $\pi\pi$ amplitudes at $m = m_\rho$. It is seen not to go through 0 at $t = 0$. The solid curve on this figure is the result of a Monte Carlo run, with 400 000 events, and gives the DCS valid for the selection of events used. Thus, above $|t| \gtrsim 7\mu^2$, one can see the effect of the background of the other processes, such as three-body phase space and N^* production. The three arrows indicate the kinematic limits at 2.77 GeV/c in t for m = 650, 773.5, and 900 MeV, namely $t = -0.31$, -0.68, and $-1.34\ \mu^2$, respectively. In Figs. 5 and 6, the solid curves were again obtained in the Monte Carlo run.

In the cases of the DCS multiplied by $\langle Y_{10}\rangle$ and $\langle Y_{20}\rangle$, respectively, the dotted curves are the computed values, using expressions which may be derived trivially from formulas (13) and (14) at the ρ mass. As in Fig. 4 they diverge from the solid curves in the region of the Chew-Low boundary and, of course, below the kinematic limit in t. They peak at $t = t_{\min}$ and are again seen not to vanish at $t = 0$.

Figures 4–6 give the best evidence for the validity of the FM parametrization. However, in view of the apparently large number of parameters, presented in Table I, that are used in the over-all maximum-likelihood fit, it is worth making plain which, and how many, parameters were required just to fit the plots presented in Figs. 4–6. Evidently the $3\Gamma_i^{s,p}$ parameters are necessary. Of the exponential slope parameters A_0^p and A_1^p may be taken as true parameters. Since we are averaging over the dipion mass, the phase-shift parameters do not enter as very sensitive parameters. Lastly, since we did not attempt to carry out an absolute determination of cross section, we have one normalization in Fig. 4. It is fair to say that six parameters were required to fit Fig. 4, and five for Figs. 5 and 6. The χ^2's that are obtained with the solid curves on the basis of the error bars, which are statistical only, range from 24 in the case of $\langle Y_{11}\rangle$ to 34. Confidence levels for the fits to these distributions are in the range 2–15% for 20 degrees of freedom.

In Figs. 7–9, we try to investigate the mass dependence within the 650–900-MeV mass band. We have used our 2.77-GeV/c data, together with the events from the data compilation range 1.7–3.2 GeV/c, and divided the total sample of events into three approximately equal subsamples, with m in the ranges 650–750, 750–800, and 800–900 MeV. We have already remarked that, in the main, data from the compilation are compatible with the 2.77

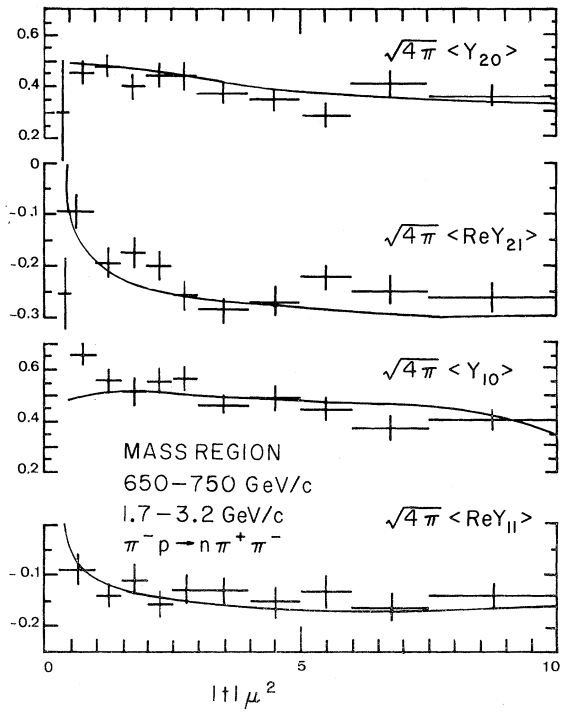

FIG. 7. Experimental values of $\sqrt{4\pi}\langle Y_{lm}\rangle$ for the mass region 650–750 MeV. The data are from the world compilation 1.7–3.2 GeV/c plus the present experiment at 2.77 GeV/c. The curves are the values calculated with the FM parametrization and the parameters obtained in the fit for m = 700 MeV and P_{lab} = 2.77 GeV/c.

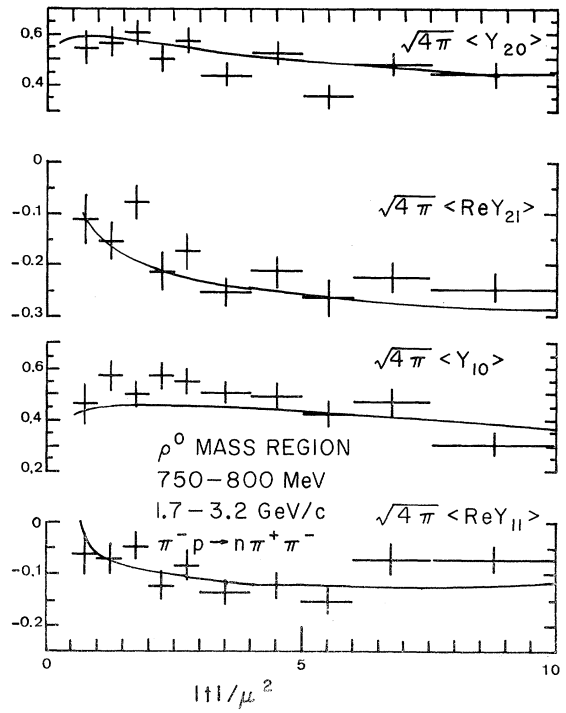

FIG. 8. Experimental values of $\sqrt{4\pi}\langle Y_{lm}\rangle$ for the ρ^0 mass region 750–800 MeV. The data are from the world compilation 1.7–3.2 GeV/c plus the present experiment at 2.77 GeV/c. The curves are the values calculated with the FM parametrization and the parameters obtained in the fit for m = 773 MeV and P_{lab} = 2.77 GeV/c.

GeV/c, although we expect discrepancies when adding together all the data for $\langle Y_{10}\rangle$.

$\langle Y_{20}\rangle$. Inspection of the three figures shows this moment increases with m, as can be expected. The three curves which are computed at the three central mass values, i.e., 700, 773.5, and 850 MeV for P_{lab}=2.77 GeV/c, also display this tendency. The fits at the two lower mass selections are satisfactory.

$\langle Y_{21}\rangle$. There, the tendency is for Re$\langle Y_{21}\rangle$ to decrease as we go to higher mass values. There is a tendency for the model to predict too large an effect for $-t \sim 5$–$10\ \mu^2$. Again, this is worst for the highest mass sample. Attempts to put a variation of the p-wave parameters Γ_i^p with m, of the form

$$\Gamma_i^p(m) = \left(\frac{t_{\min}}{t_{\min}(\rho)}\right)^{1/2} \frac{m}{m_\rho}\,\frac{m_\rho^2-\mu^2}{m^2-\mu^2}\,\Gamma_i^p(m_\rho) \qquad (18)$$

(see for example Ref. 13), tended to change things for the worse, i.e., the tendency was for Re$\langle Y_{21}\rangle$ to be increased with m and $\langle Y_{20}\rangle$ to be decreased, compared with the values calculated with fixed parameters. In any case, the log likelihood was much less.

$\langle Y_{10}\rangle$. In view of the mixture of beam momenta and in the light of the difficulties mentioned above, it is sensible not to attempt to draw any conclusion from the curves computed.

$\langle Y_{11}\rangle$. The statistics are good enough for us to say that, although the quantity Re$\langle Y_{11}\rangle$ is small, it can be well represented by our model.

The conclusion that can be drawn from the three figures is that even at its worst, the FM formulation can provide predictions of the measured quantities of the right orders of magnitude over a wide mass and over-all energy range.

If it is now accepted that the description is a good one, we may return to the question of the physical significance of the $\Gamma_i^{s,p}$. As can be seen from the formulas (3)–(6) for the helicity amplitudes, they are the coefficients of the first-order correctional terms to OPE. We have seen that as a result of their being nonzero, the DCS and related functions vanish at slightly positive, i.e., nonphysical, values of t. It is convenient to use the expressions for F_0, F_1, and F_2 to compute roughly where these functions vanish: e.g., for F_0 by neglecting Γ_0^s, it can be seen that $F_0(m_\rho, t_0) = 0$ for $t_0 = 0.14\mu^2$. By differentiating formula (12) and making the approximation that Γ_0^s and the error

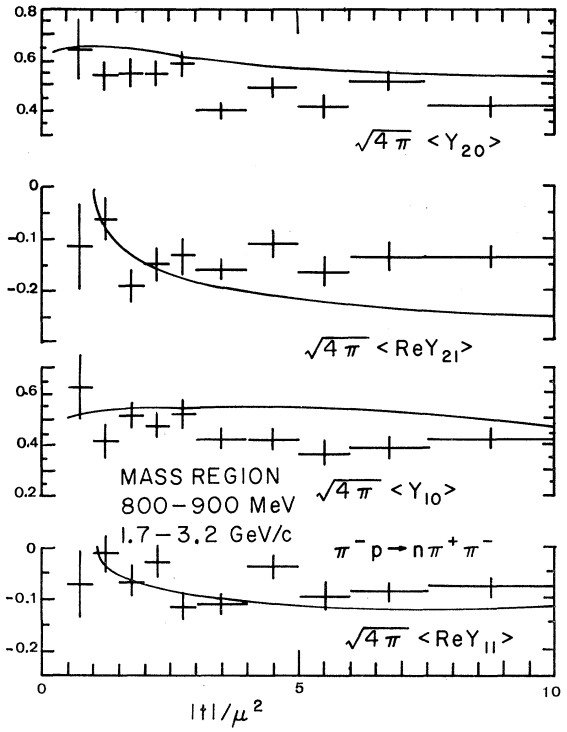

FIG. 9. Experimental values of $\sqrt{4\pi}\langle Y_{lm}\rangle$ for the mass region 800–900 MeV. The data are from the world compilation 1.7–3.2 GeV/c plus the present experiment at 2.77 GeV/c. The curves are the values calculated with the FM parametrization and the parameters obtained in the fit for m = 850 MeV and P_{lab} = 2.77 GeV/c.

in Γ_1^p are both small and can be neglected, we find that

$$\Delta t_0 \approx 2\Delta\Gamma_0^p, \quad \Delta t \sim 0.02\ \mu^2 .$$

In Fig. 10, we present the graphs of the three functions $F_l(m_\rho, t)$ as functions of t. Although the functions are slow smooth curves, they appear distorted because of our choice of scale. Within the dotted square, i.e., for $|t|/\mu^2 = 0.1$ and $|F_l| < 0.6$ mb the scale is linear. In the four large corners it is log-log and elsewhere log-linear. In this way, we have the advantage of the log-log scale without problems at the origin. The two hatched areas give an idea of the effect of the errors on the $\Gamma_l^{s,p}$ on the position of F_0. We have taken advantage of the work of BLR to assume that the intercept at $t = \mu^2$ is the value of $-\sigma_{\pi\pi}(m_\rho)$. The figure makes the following facts obvious: F_0 and, to a lesser degree of confidence, F_1 and F_2 do not pass through 0 at $t = 0$. The value of $F_0(m_\rho, 0)$ is of the order 15–20 mb. Furthermore, F_1 and F_2 do not vanish at the same value as does F_0, i.e., t_0, and this accounts for the singularities appearing in the ratios $\langle Y_{10}\rangle = F_1/F_0$ and $\langle Y_{20}\rangle = F_2/F_0$.

In Ref. 9, BLR have determined $\pi\pi$ phase shifts using evasive extrapolation, i.e., using the functions $F_l(m, t)/t$. It is likely that this error is not as bad as it appears, since from the point of view of the final uncertainty in the value of a phase shift, it matters little whether one extrapolates F_l/t or the more correct $F_l/(t+\epsilon)$ where ϵ is of the order of 0.1–$0.3\,\mu^2$ – and in any case can be a further parameter in a fit.

To illustrate this last point, in Fig. 11 we show the curve obtained with our values for $\Gamma_l^{s,p}$ for the function $F_0(m, 0)$ as a function of m. The data points are those of BLR[14] and were obtained by extrapolation of $F_0(m, t)$ after mapping. If it is agreed that the least one gets out of the FM parametrization is the shape of the curve, then our curve is seen to overestimate the function. A χ^2 comparison with the BLR assumption that $F_0(m, 0) = 0$, of 25 : 9 favors the null hypothesis. However, the error bars shown take no account of any possible systematic error in the normalization. If Γ_0^p were taken with a value -0.03, giving a maximum value at the ρ mass of about 15 mb, the curve would fit the points optimally in the 700–800-MeV region. The small quantity ϵ is a function of the mass, $\epsilon(m)$, and would be easy to adjust so that all three functions $F_l(m, t)$ have a t intercept following a curve similar to the one we have shown.

We may also mention here the wider theoretical significance of the $\Gamma_l^{s,p}$ parameters. In Ref. 13 there is some discussion of what light they throw on the theories of absorption (OPEK)[11] and vector dominance (CS).[15] A slightly different form of the p-wave parameters is used, namely,

$$\gamma_0^p = \sqrt{2}\,\Gamma_0^p k_0/[-t_{\min}(\rho)]^{1/2}, \tag{19}$$

$$\gamma_1^p = 2\sqrt{2}\,\Gamma_1^p k_0/[-t_{\min}(\rho)]^{1/2}. \tag{20}$$

Our values of $\gamma_0^p = 0.29 \pm 0.04$ and $\gamma_0^p = 1.065 \pm 0.02$ are to be compared with the OPEK predictions of 0.26 and 1.14, respectively. The agreement is good. However, we are also compatible with the CS prediction of 0.97 for the latter parameter. The conclusion may be drawn, as in Ref. 13, that the theory of absorption, as used, for example, by Williams[10,11] and the vector dominance model for photoproduction[15] are valid descriptions of the data at low t. Either of the models may be broached in terms of the FM parametrization, which is then a more general and certainly less model-dependent way of fitting the data. Thus we may be confident of being able to fit the data of Baillon *et al.*[10] as well as reproducing the calculation of Williams with a suitable choice of parameters.

In conclusion, then, we have used a formalism based on a reasonable assumption of the behavior of the helicity amplitudes. The parametrization is

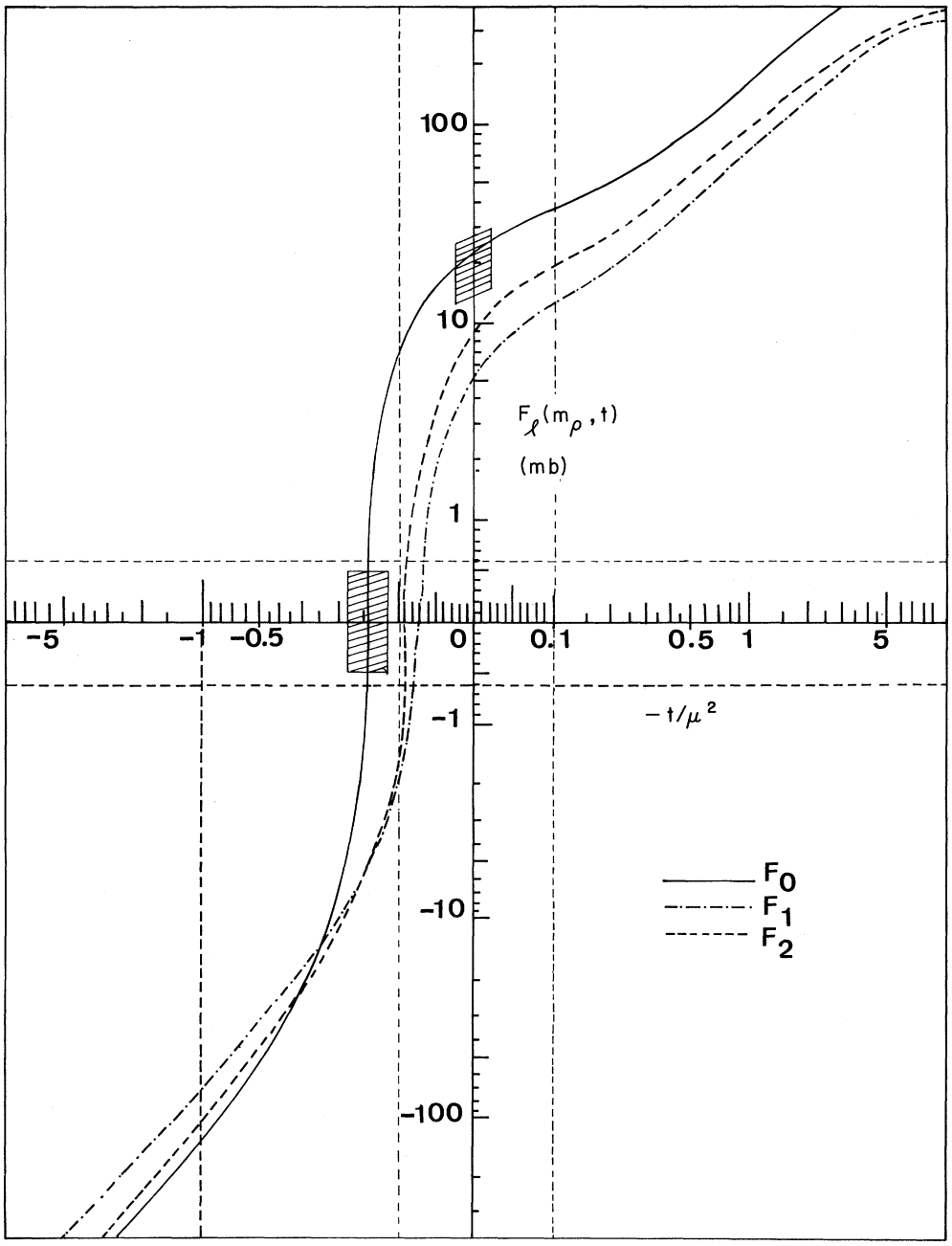

FIG. 10. Graphs of the three "off-shell" functions F_0, F_1, and F_2 computed at m_ρ. The scale is linear for $|F_l| < 0.6$ mb and $|t|/\mu^2 < 0.1$ and otherwise logarithmic. The hatched regions show the estimated error on F_0. The position of the pion pole is indicated.

phenomenological. It lends itself well to fitting the data in hand and provides a criticism as well as a measured justification for some already known methods of extrapolation. In the sense that one must accept the form of the amplitudes in the physical region in order to believe our results in the unphysical region, i.e., that $F_l \neq 0$ at $t = 0$, we ourselves are performing an extrapolation. However this was not the emphasis in the paper. Use of the FM formalism for extrapolation would be best carried out on a mass band by mass-band basis – with the three $\Gamma_i^{s,p}$ determined explicitly for each mass band. Lastly we have mentioned that our results support the conclusion of Ref. 13, namely that the FM parametrization might well follow from two simple models of the reaction.

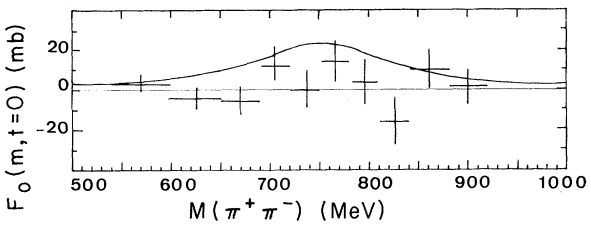

FIG. 11. Values of $F_0(m_0, 0)$ obtained by BLR (Ref. 14) by extrapolation after mapping. The curve is calculated with the FM parametrization.

TABLE II. Apportionment of the reaction $\pi^- p \to n\pi^+\pi^-$ at 2.77 GeV/c among the various processes, resonant and otherwise. Breit-Wigner parameters shown, where appropriate.

Process	Proportion	Mass (GeV)	Width (GeV)
$n\rho^0$	0.56 ± 0.02	0.7735 ± 0.001	0.17835 ± 0.0025
$n(\pi\pi)_s$	0.06 ± 0.01	...	...
nf^0	0.10 ± 0.03	1.2610 ± 0.010	0.130 ± 0.025
$n\pi^+\pi^-$	0.20 ± 0.03	...	...
$\Delta^-\pi^+$	0.02 ± 0.002	1.2195 ± 0.015	0.0745 ± 0.015
$\Delta^+\pi^-$	0.01 ± 0.003	1.2195 ± 0.015	0.0745 ± 0.025
$N^{*+}(1650)\pi^-$	0.02 ± 0.003	1.653 ± 0.20	0.062 ± 0.015
$N^{*+}(1520)\pi^-$	0.025 ± 0.005	1.533 ± 0.010	0.085

OTHER PROCESSES

We complete the discussion of the fit by listing explicitly the other processes in the fit. In Table II they are presented together with the values and errors of the appropriate parameters.

(i) The proportion of ρ produced also includes 0.075 ± 0.01 of ρ produced at larger values of t and which has a t dependence of the form te^{at} where $a \sim 1$ GeV^{-2}. With this parametrization, we know that it has zero contribution at $t = 0$ and therefore cannot invalidate our results obtained above.

(ii) We have included a term describing f^0 production. In view of the smaller rate of production of the f^0 and the number of additional helicity amplitudes that the introduction of d waves would entail, we have not included the f^0 in the FM parametrization.

(iii) Three-body phase-space contributes about 20% of the events.

(iv) Lastly we have various isobar effects. The Δ^- (1238) and N^{*+}(1650) are evidently required by inspection of the histograms in Fig. 12. Other effects in the $n\pi^+$ system were only introduced after all the other contributions were optimized and it was seen that in contrast to the $n\pi^-$ spectrum the $n\pi^+$ was still badly reproduced. The fit to this spectrum remains unsatisfactory. One interesting feature of this spectrum may be the hole centered at ~1900 MeV. No allowance was made for the pro-

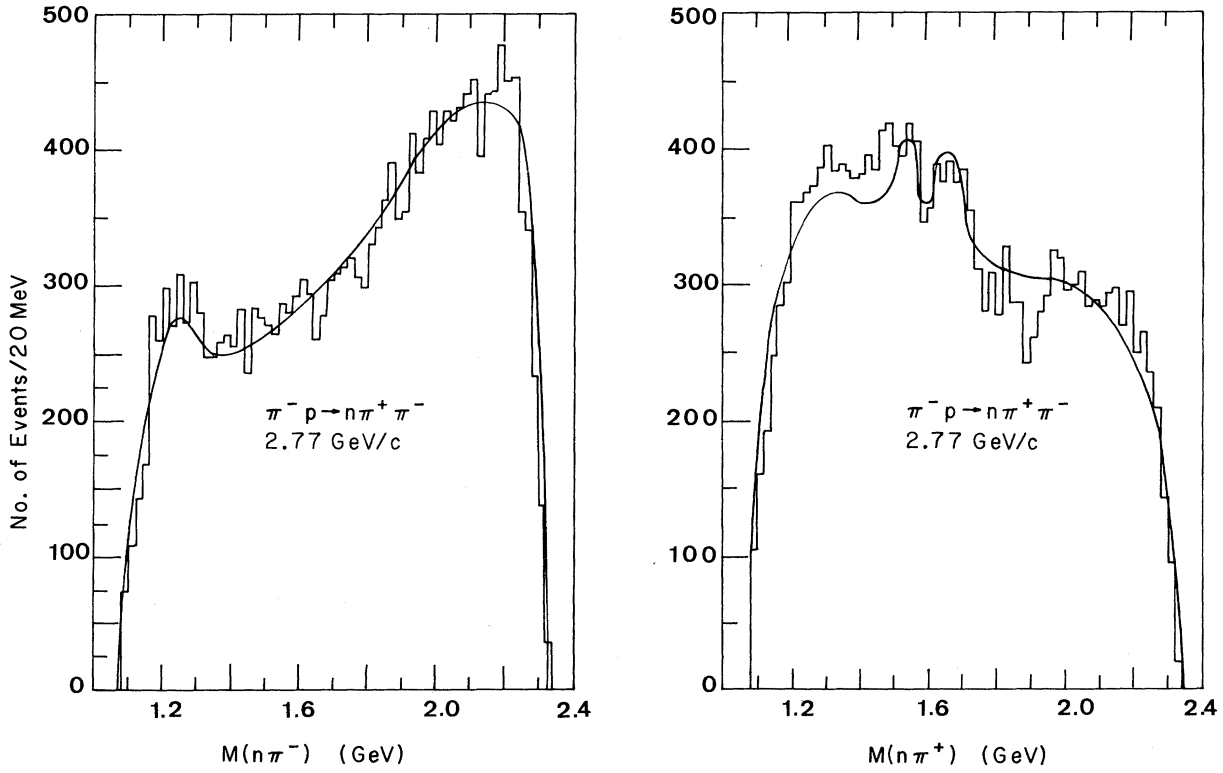

FIG. 12. $n\pi^-$ and $n\pi^+$ mass spectrum for all events. Curves are taken from Monte Carlo simulations of the fit with the parameters shown in Table II.

duction and decay angular dependences of these nucleon resonances – although it has been observed that the $\Delta^-(1238)$ appears to be formed predominantly in the forward direction.[2] This experimental fact is, at present, not well explained. We, for example, were not able to reproduce the effect in our Monte Carlo sample, after putting the dipion decay distributions into our fit. Possibly $n\pi^\pm$ amplitudes interfering with $\pi^+\pi^-$ amplitudes are necessary; we did not introduce this for practical reasons.

ACKNOWLEDGMENTS

The author would like to extend his appreciation to Professor A. Berthelot and Professor A. Rogozinski for the opportunity of working at the C.E.N. at Saclay. Further he would like to thank Dr. Marcel Froissart for the hospitality and congenial conditions afforded him at the D. Ph. P.E. In particular, he is deeply indebted to Dr. J. P. Baton and Dr. Georges Laurens of whose experiment he has taken such full advantage and with whom he has had many stimulating discussions. He would like to thank Monique Neveu among others for her interest in the work, and Dr. R. Barloutaud and Dr. David Morgan (R.H.E.L.) for reading the original manuscript.

APPENDIX A: RELATIONSHIPS BETWEEN MEAN MOMENTS AND DENSITY-MATRIX ELEMENTS

$\langle Y_{10}\rangle$,

$$2\rho_{00}^{10} = \sqrt{4\pi}\langle Y_{10}\rangle . \tag{A1}$$

Asymmetry parameter

$$\alpha = (F-B)/(F+B)$$
$$= (\tfrac{3}{4})^{1/2}(\sqrt{4\pi}\,\langle Y_{10}\rangle) . \tag{A2}$$

From this relationship we see that the maximum value of $\sqrt{4\pi}\langle Y_{10}\rangle$ is $(\frac{4}{3})^{1/2} = 1.1547$.

$\langle Y_{11}\rangle$,

$$2\rho_{10}^{10} = \sqrt{4\pi}\langle Y_{11}\rangle . \tag{A3}$$

$\langle Y_{20}\rangle$,

$$(\tfrac{4}{3})^{1/2}(\rho_{00}^{11} - \rho_{11}^{11}) = \sqrt{4\pi}\langle Y_{20}\rangle . \tag{A4}$$

$\langle Y_{21}\rangle$,

$$(\tfrac{12}{5})^{1/2}\rho_{10}^{11} = \sqrt{4\pi}\langle Y_{21}\rangle . \tag{A5}$$

$\langle Y_{22}\rangle$,

$$(\tfrac{12}{5})^{1/2}\rho_{1-1}^{11} = \sqrt{4\pi}\langle Y_{22}\rangle . \tag{A6}$$

---

*Present address: Dept. of Physics and Astronomy, Tel-Aviv University, Ramat-Aviv, Israel.

[1]D. S. Beder, Phys. Rev. 149, 1203 (1966); J. J. Sakurai, in *Fourth International Symposium on Electron and Photon Interactions at High Energies, Liverpool, 1969,* edited by D. W. Braben and R. E. Rand (Daresbury Nuclear Physics Laboratory, Daresbury, Lancashire, England, 1970).

[2]G. L. Kane and M. Ross, Phys. Rev. 177, 2353 (1969).

[3]J. P. Baton and G. Laurens, Nucl. Phys. B21, 551 (1970).

[4]J. H. Friedman, Alvarez Programming Group Note P-156 (MURTLEBERT), 1966 (unpublished).

[5]F. James, CERN Program Library W505 (FOWL), 1968 (unpublished).

[6]J. H. Friedman and A. Rittenberg, Alvarez Programming Group Note P-171 (KIOWA), 1968 (unpublished).

[7]C. D. Froggatt and D. Morgan, Phys. Rev. 187, 2044 (1969).

[8]J. H. Scharenguivel, L. J. Gutay, D. H. Miller, R. L. McIlwain, F. T. Meiere, D. Morgan, L. D. Jacobs, S. Marateck, C. D. Froggatt, D. Huwe, and E. Marquit, Phys. Rev. Letters 24, 332 (1970).

[9]J. P. Baton, G. Laurens, and J. Reignier, Phys. Letters 33B, 528 (1970).

[10]P. Baillon, F. Bulos, R. K. Carnegie, G. E. Fischer, E. E. Kluge, D. W. G. S. Leith, H. L. Lynch, B. Ratcliff, B. Richter, H. H. Williams, and S. H. Williams, Phys. Letters 35B, 453 (1971).

[11]P. K. Williams, Phys. Rev. D 1, 1312 (1970).

[12]See, for example, the selective compilation of $\pi^- p \to \pi\pi N$ events from hydrogen bubble chambers, L. D. Jacobs, M. Roos, and S. Santiago, CERN Report No. CERN/HERA 71/1, 1971 (unpublished), for a complete list of references.

[13]C. D. Froggatt and D. Morgan, Phys. Letters 33B, 582 (1970).

[14]J. P. Baton, G. Laurens, and J. Reignier, Phys. Letters 33B, 525 (1970).

[15]C. F. Cho and J. J. Sakurai, Phys. Letters 30B, 119 (1969); Phys. Rev. D 2, 517 (1970).